ATTORNEY'S DOCKET NUMBER: 0492611-0375 (MIT 8802)

IN THE UNITED STATES PATENT AND TRADEMARK OFFICE

Applicant:	Kamm *et al.*	Examiner:	Mathew, F. C.
Serial No.:	09/815,528	Group Art Unit:	3764
Filed:	March 23, 2001		
For:	METHOD AND APPARATUS FOR STIMULATING ANGIOGENESIS AND WOUND HEALING BY USE OF EXTERNAL COMPRESSION		

Commissioner for Patents
P.O. Box 1450
Alexandria, VA 22313-1450

Declaration under 37 C.F.R. § 1.131

I, Roger D. Kamm, declare as follows:

1. I am currently a Professor in the Department of Mechanical Engineering and the Biological Engineering Division at the Massachusetts Institute of Technology, Cambridge, Massachusetts. My research focuses on biomedical fluid dynamics, computational fluid dynamics, cell mechanics, and biomedical engineering. A copy of my curriculum vitae is attached as **Exhibit A**.

2. I am a co-inventor of the subject matter disclosed and claimed in United States Patent Application Serial Number 09/815,528, filed March 23, 2001, and entitled "Method and Apparatus for Stimulating Angiogenesis and Wound Healing by Use of External Compression" (the '528 application).

3. This declaration is presented for the purpose of removing from consideration by the Examiner the reference by Lewis (U.S. Patent 6,620, 116 (the '116 patent), filed December 8, 2000, and issued September 16, 2003).

4. On a date before December 8, 2000, the filing date of the '116 patent, Dr. Jonathan Gertler and I conceived of a system for stimulating angiogenesis and promoting wound healing by using external graded sequential compression to induce a change in the shear stress on the

endothelial cells of a patient's vasculature. The endothelial cells experiencing a change in shear stress secrete factors which stimulate angiogenesis and/or promote wound healing.

5. **Exhibit B** is the completed MIT Technology Disclosure form submitted by myself and Dr. Gertler to the MIT Technology Licensing Office describing the invention in the '528 application. Attached to the disclosure form is a manuscript entitled "Numerical Simulation of Enhance External Counterpulsation. Part II: Hemodynamic Results," which describes a computational model of the inventive system. The first page of the disclosure form bears a date prior to December 8, 2000; however, this date has been redacted.

6. I declare that all statements made herein of my own knowledge are true, and that those statements made on information and belief are believed to be true; and further that these statements were made with the knowledge that willful, false statements and the like are made punishable by fine or imprisonment, or both, under Section 1001 of Title 18 of the United States Code and that such willful, false statements may jeopardize the validity of the '528 application or any patents that may issue thereon.

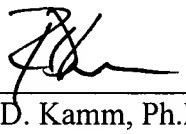

Roger D. Kamm, Ph.D.

June 23, 2004

Date

Exhibit A

ROGER D. KAMM

Curriculum Vitae

PERSONAL INFORMATION:

Date of Birth:	October 10, 1950
Office Address:	Massachusetts Institute of Technology
	77 Massachusetts Avenue
	Room 3-260
	Cambridge, Massachusetts 02139
Telephone:	(617) 253-5330
FAX:	(617) 253-8559
e-mail:	rdkamm@mit.edu
Home Address:	31 Nonesuch Road
	Weston, Massachusetts 02193

PROFESSIONAL EXPERIENCE:

1998-	:	Professor of Bioengineering, M.I.T.
1995-	:	Lecturer on Medicine, Harvard Medical School
1994-	:	Associate Director, Center for Biomedical Engineering, M.I.T.
1992-1994	:	Co-Director: Program in Biomedical Engineering, M.I.T.
1988-	:	Professor of Mechanical Engineering, M.I.T.
1988-	:	Professor of Health Sciences and Technology, M.I.T. and Harvard University
1981-1988	:	Associate Professor of Mechanical Engineering, M.I.T.
1986-1987	:	Senior Visiting Scientist, University of Cambridge, Department of Applied Mathematics and Theoretical Physics. Visiting Fellow, Clare Hall, University of Cambridge.
1978-1981	:	Assistant Professor of Mechanical Engineering, M.I.T.
1977-1978	:	Lecturer and Research Associate in the Department of Mech. Engineering, M.I.T.
1977	:	Instructor, M.I.T.

EDUCATION:

MASSACHUSETTS INSTITUTE OF TECHNOLOGY, Cambridge, MA
Ph.D. in Mechanical Engineering, May 1977
MASSACHUSETTS INSTITUTE OF TECHNOLOGY, Cambridge, MA
S.M. in Mechanical Engineering, August 1973
NORTHWESTERN UNIVERSITY, Evanston, Illinois
B.S. in Mechanical Engineering, June 1972

HONORS, AWARDS AND SCHOLARSHIPS:

Harry Coulby Scholarship Award (1968-1972)
NSF Traineeship (1972-1973)
NIGMS Graduate Fellowship Award (1974-1977)
Tau Beta Pi, Pi Tau Sigma, Sigma Xi
Graduate Student Council Teaching Award (1983)
American Inst. of Medical and Biological Engineering (Founding Fellow) (1993)
Class of 1960 Award (for development of the Undergraduate Minor in Biomedical Engineering) (1999)
Everett Moore Baker Memorial Award for Excellence in Undergraduate Teaching (2001)
Cambridge/MIT Fellow (2001)
Southwest Mechanics Lecturer (2002)
Eschbach Distinguished Visiting Scholar Award, Northwestern University (2002)
Who's Who in America, Who's Who in American Education, Who's Who in Science and Technology

PROFESSIONAL SOCIETIES:

American Institute for Medical and Biological Engineering (Founding Fellow)
American Society of Mechanical Engineering
Biomedical Engineering Society (Fellow)
American Physiological Society

OTHER PROFESSIONAL ACTIVITIES:

Biomedical Engineering Society; Chair, Awards Committee (1989-91)
Biomedical Engineering Society; Board of Directors (1994-1997)
ASME Journal of Biomechanical Engrg., Associate Editor (1990-1996)
American Heart Association; Research Peer Review Committee (1991-1993)
NHLBI, NIEHS, NASA, NSF; Review Committees (1988-present)
Journal of Fluids and Structures, Associate Editor (1993-present)
Methods in Cell Science, Editorial Board (1995-present)
US National Committee on Biomechanics; executive committee (1997-present); secretary (2000-present)
World Council on Biomechanics (1998-present); vice chair (2002-2006)
External Review Board, City University of New York, Biomedical Engineering Doctoral Program (1999)
External Advisory Board, Northwestern University, Dept. of Biomedical Engineering (2000-present)
Summer Bioengineering Conference, Conference Chair, 2001
Biomechanics and Modeling in Mechanobiology, Editorial Board, 2001-present)
External Review Board, Pennsylvania State University, Dept. of Biomedical Engineering (2003)
External Review Board, Duke University, Dept. of Biomedical Engineering (2003)

RECENT INVITED LECTURES (past year)

Meeting on Protein Folding and Self-Assembly, Crete, *Self-Assembling Peptide Biomaterials*, July, 2001.
Georgia Tech, Atlanta, GA, *Cellular mechanics and its role in biological function: Studies in neutrophil margination, deformation, and microstructure*, September, 2001.
First International Conference on Information in Fluid Science. Sendai, Japan, *Multi-Scale Simulation in Biological Systems,* October, 2001.
University of Nottingham, UK, *Some intriguing problems in molecular and cellular mechanics*, October, 2001
University of Cambridge, UK, *Mechanics of the cytoskeleton and other self-assembled protein networks*, October, 2001
Southwest Mechanics Lecture Series, January, 2002: *Biological Nano-Mechanics: From Cells to Proteins*
Tulane University, New Orleans, Southern Methodist University, Dallas, University of Houston, Houston, University of Oklahoma, Norman
Northeastern University, *Biomechanics of Cells and Molecules*, January, 2002.
Rensselaer Polytechnic Institute, *Biological Nano-Mechanics*, February, 2002.
Florida International University, *Mechanics of Self-Assembling Peptides and their Use as a Biomaterial*, March, 2002.
University of Vermont, *Cellular Biomechanics – Bridging between Continuum and Molecular Models*, March, 2002.
Northwestern University (The Eschbach Distinguished Visitor Lecture), *Cellular Biomechanics – Bridging between Continuum and Molecular Models*, April, 2002.
DuPont TechCon, Delaware, *Self-assembling peptide biomaterials*, May, 2002.
US National Conference on Theoretical & Applied Mechanics, Blacksburg, Virginia, *Correlations Between Fluid Shear Stress or Tissue Stress and Histological Markers in Advanced Carotid Artery Disease,* June, 2002.

RECENT PUBLICATIONS

Huang, Y., Doerschuk, C.M., Kamm, R.D. Computational modeling of RBC and neutrofil transit through the pulmonary capillaries. J Appl Physiol, 90:545-564, 2001.

Huang H, Virmani R, Younis H, Burke AP, Kamm RD, Lee RT. The Impact of Calcification Upon the Biomechanical Stability of Atherosclerotic Plaques. Circulation, 103:1051-1056, 2001.

Ozawa, E.T., K.E. Bottom, X. Xiao, and R.D. Kamm. Numerical simulation of enhanced external counterpulsation. Ann Biomed Eng. 2001 Apr;29(4):284-97.

Swartz, MA, Tschumperlin, DJ, Kamm, RD, Drazen, JM. Mechanical stress is communicated between different cell types to elicit matrix remodeling. PNAS, 98:6180-5, 2001.

Huang H, Kamm RD, So PT, Lee RT. Receptor-based differences in human aortic smooth muscle cell membrane stiffness. Hypertension. 2001;38:1158-61.

Heldt, T., Shim, E.B., Kamm, R.D., Mark, R.G. Computational modeling of cardiovascular response to orthostatic stress. Am J Physiol, 92(3): 1239-54, 2002.

Heldt, T., Shim, E.B., Kamm, R.D., Mark, R.G. Computational model of cardiovascular function during orthostatic stress. Comput Cardiol, 27: 777-80, 2002.

Caplan, MR, Schwartzfarb, EM, Zhang, S, Kamm, RD, Lauffenburger, DA. Control of self-assembling oligopeptide matrix formation through systematic variation of amino acid sequence. Biomaterials, 23:219-227, 2002.

Kamm, RD. Cellular fluid mechanics. Ann Rev Fluid Mech, 34:211-32, 2002.

Powers MJ, Domansky K, Mofrad, MRK, Kalezi A, Capitano A, Upadhyaya A, Kurzawaski P, Wack KE, Stolz DB, Kamm RD, Griffith LG. A microfabricated array bioreactor for perfused 3D liver culture. Biotechnol Bioeng, 78:257-269, 2002.

McKay, KO, Wiggs, BR, Pare, PD, Kamm, RD. The zero stress state of intra- and extraparenchymal airways from human, pig, rabbit and sheet lung. J Appl Physiol, 92(3): 1239-54, 2002.

Caplan MR, Schwartzfarb EM, Zhang S, Kamm RD and Lauffenburger DA. Effects of systematic variation of amino acid sequence on the mechanical properties of a self-assembling, oligopeptide biomaterial. J Biomaterials Sci, 13(3): 225-236, 2002.

Xiao X, Ozawa ET, Hwang Y, Kamm RD. Model-based assessment of cardiovascular health from noninvasive measurements. Ann Biomed Eng, 30(5):612-23, 2002.

Dai G, Tsukarov O, Chen M, Gertler JP, Kamm RD. Nitric oxide production by cultured human vein endothelial cells: response to in vitro simulation of external pneumatic compression. Am J Physiol Heart Circ Physiol. 282(6):H2066-75, 2002.

Marini DM, Hwang W, Lauffenburger DA, Zhang S, Kamm RD. Left-handed helical ribbon intermediates in the self-assembly of a β-sheet peptide. Nano Letters, 2(4): 295-299, 2002.

Hrousis CA, Wiggs BJR, Drazen JM, Parks DM, Kamm RD. Mucosal folding in biologic vessels. J Biomech Eng, 124:334-341, 2002.

Napadow V, Kamm RD, Gilbert J. A biomechanical model of sagittal tongue bending. J Biomech Eng., 124(5): 547-556, 2002.

Shim, EB, Kamm RD. Numerical simulation of steady flow in a compliant tube or channel with tapered wall thickness. J Fluids Structures, in press.

Bathe, M. Shirai, A, Doerschuk, CM, Kamm, RD. Neutrophil transit times through pulmonary capillaries: The effects of capillary geometry and fMLP-stimulation. Biophys. J., in press, 2002.

Williamson SD, Lam Y, Younis HF, Huang H, Patel S, Kaazempur-Mofrad MR, Kamm RD. On the sensitivity of wall stresses in diseased arteries to variable material properties, J Biomech Eng, in press.

Hwang W, Marini DM, Kamm RD, Zhang S. Supramolecular structure of helical ribbons self-assembled from a b-sheet peptide. J Chem Phys, in press.

RECENT INDUSTRIAL INTERACTIONS (past two years)

APEX Medical (Scientific Advisory Board)
Mitsubishi Electric (medical products) (Consultant)
Percardia, Inc. (Consultant, Scientific Advisory Board)
Cardiovascular Technologies (Co-founder)
Embolic Protection, Inc. (Consultant, Scientific Advisory Board)
STD Manufacturing (Consultant)
Aircast, Inc. (Research sponsor)
Hale and Dorr (Consultant)
MyoMend, Inc. (Scientific Advisory Board)

RESEARCH INTERESTS

Cell mechanics and mechanotransduction

Cytoskeletal mechanics and computational modeling of cell deformations and force transmission through the cell.

Measurements of intracellular strain fields due to forces applied by adherent beads.

Transduction of mechanical signals by protein conformational changes.

Cardiovascular fluid dynamics

Numerical simulation of cardiovascular flows including the mechanics of the normal and pathologic arterial wall, heart assist and total artificial heart, flows induced by external compression, external pneumatic compression and external cardiac assist.

The effects on endothelial function of shear stress in terms of altering fibrinolytic tendencies, inducing the adhesion of monocytes in the vicinity of an atherosclerotic lesion, and the stimulation of macrophages by mechanical stress of the arterial wall.

Biomaterials

Development of functionalized scaffold for tissue engineering based on self-assembled peptide hydrogels.

Design of peptide matrices for studies of angiogenesis and cardiac tissue engineering.

Respiratory mechanics and fluid dynamics

Studies of the airway wall mechanics during bronchoconstriction in normal and asthmatic airways and the potential role of stress-induced remodeling.

Modeling of the flow of red blood cells and neutrophils through the lung, and the process by which neutrophils tend to accumulate in the pulmonary vasculature.

Biomaterials

Development of new oligopeptide biomaterials that self-assemble under physiologic conditions and can be used as scaffolds for tissue implants and drug delivery.

Studies into the relationship between peptide sequence and the process of self-assembly.

CURRENT RESEARCH SUPPORT

Agency	Grant Title	Period Covered
NHLBI	*Numerical analysis of flow and tissue deformation in the atherosclerotic artery*	10/1/98 – 9/31/02
NASA	*Computational Models of the Cardiovascular System*	10/1/01 – 9/31/03
Aircast	*Angiogenesis by External Compression*	9/1/95 - continuing
DuPont/MIT Alliance	*Micromechanical Properties of Biopolymers: New Measurement Instrumentation with Application to Self-Assembling Peptide Nanofiber Materials*	9/1/00 - 8/31/02
NHLBI	*Mechanotransduction in Cardiovascular Cells (PPG)*	9/28/01-9/31/06
NHLBI	*In-Situ Measurement of Plaque Biomechanical Properties*	3/1/02-2/28/-05

BRIEF NARRATIVE AND CURRENT INTERESTS

Roger D. Kamm is author or co-author of over 110 papers in refereed journals in the fields of cardiovascular, respiratory, and ocular physiology and engineering. Recent interests have focused on cardiovascular issues with an aim toward melding computational approaches with cell and molecular biology. Most of Kamm's research is performed with support from four current NIH grants, with additional support coming from NASA, DARPA, an industrial consortium, and two industrial sponsors.

Dr. Kamm holds 4 patents in the medical device field with 2 patents pending. He co-founded CardioVascular Technologies, Inc., which emphasized new approaches to non-invasive or minimally-invasive treatment of vascular disease. He maintains an active consulting practice in the broad area of biomedical devices and the use of computational modeling in medicine.

Dr. Kamm has also been actively instrumental in the education of students in bioengineering and biomechanics. He was one of three faculty to develop the Undergraduate Minor in Biomedical Engineering (1995) at MIT, and chaired the committee to initiate the Master of Engineering in Biomedical Engineering (2000). With two colleagues, he developed a new subject in *Molecular, Cellular and Tissue Biomechanics* for which he is currently writing a textbook with sponsorship of the Whitaker Foundation. He was the recipient of the Everett Moore Baker Memorial Award, the highest, Institute-wide teaching award selected by students.

Exhibit B

M.I.T. TECHNOLOGY DISCLOSURE

When completed submit to:
Technology Licensing Office
Room NE25-230, 253-6966

Case No. (this space for TLO use only)
8802

Instructions on reverse

1. TITLE OF INVENTION

A method and apparatus for stimulating angiogenesis and wound repair by use of external compression

2. PLEASE ATTACH DESCRIPTION OF TECHNOLOGY

3. INVENTOR(S)	POSITION	DEPARTMENT/M.I.T. ROOM NO. & EXTN.
Jonathan P. Gertler	Lecturer (MIT)	Mass. General Hospital
Roger D. Kamm	Prof.	Mech. Eng., 3-260, x3-5330

4. Was this invention developed with the use of any research grant/contract funds? YES ☒ NO ☐

CONTRACT/GRANT NO(S).	SPONSOR(S)	O.S.P. PROJECT NO(S).	PRINCIPAL INVESTIGATOR
	Aircast Corp.	6629800	R.D. Kamm

Please note that accurate and complete sponsorship information is necessary to fulfill MIT obligations under research grants and contracts.

5. If no contract or grant, was there significant use of MIT funds or facilities as defined on reverse side? YES ☐ NO ☐

6. DATES OF CONCEPTION and PUBLIC DISCLOSURE (accurate data is essential as prior disclosure may affect the possibility of obtaining patent rights)	DATE	REFERENCES/COMMENTS Please include names of periodicals/journals. (use separate sheet if necessary)
A. Date of conception of invention. Has this date been documented? If so, where?		Proposal to Aircast
B. First publication containing sufficient description to enable a person skilled in this field to understand and to make or use the invention. (include theses, and the date submitted)		Only the idea was mentioned; not much detail
C. First public oral disclosure of invention sufficient to enable a person skilled in this field to understand and to make or use the invention.	—	None
D. If unpublished and undisclosed, provide the anticipated publication or oral disclosure date and any submissions made for potential publication.		

7. Has the invention been reduced to practice? YES ☐ NO ☒ If yes, please give date of first reduction to practice _____

8. Please attach list of any commercial entities that may be interested in this invention. (provide as much detail as possible)

9. I hereby declare that all statements made herein of my own knowledge are true and that all statements made on information and belief are believed to be true.

I (We) hereby agree to assign all right, title and interest to this invention to M.I.T. and agree to execute all documents as requested, assigning to M.I.T. our rights in any patent application filed on this invention, and to cooperate with the M.I.T. Technology Licensing Office in the protection of this invention. M.I.T. will share any royalty income derived from the invention with the inventor(s) according to its standard policies.

_____ Inventor's Signature	_____ Inventor's Signature Date
31 Nonesuch Rd., Weston, MA 02493 Home Address	_____ Home Address
394-52-7946 Social Security No. (required) US Country of Citizenship	_____ Social Security No. (required) Country of Citizenship
_____ Inventor's Signature Date	_____ Inventor's Signature Date
_____ Home Address	_____ Home Address
_____ Social Security No. (required) Country of Citizenship	_____ Social Security No. (required) Country of Citizenship

Please note that Social Security number and country of citizenship are required and that the absence of this information may hinder distribution of the inventors' share of any royalties that may result from this technology. If there are more than four inventors, please attach additional form.

Technology disclosed to and understood by:
Signature of Non-Inventor Witness_____ Date_____
Name and Title of Witness (please type or print)_____
(For MIT: Principal Investigator should sign if he/she is not inventor. For Media Laboratory: Director's signature required. For Lincoln Laboratory: Division Head's signature required.)

(11/23/93)

Title of invention: A method and apparatus for stimulating angiogenesis and wound repair by the use of external compression

General purpose.-The purpose of this invention is to stimulate the patient's own arterial endothelium in a manner that leads to enhanced synthesis and secretion of angiogenic factors. These factors, released into the circulation, can subsequently lead to the growth of new blood vessels thereby alleviating the ischemia resulting from peripheral arterial disease.

Technical description. Blood flow in the vessels of the lower extremity is altered by means of pressure variations applied to of the legs by inflatable cuffs or by some other means of external compression. Pressures of a magnitude sufficient to cause collapse of the large arteries, and thereby producing reverse flow into the abdominal aorta, create large variations and changes in direction of the shear stress applied to the endothelium. Elevated levels of shear stress, and reversing shear stress, are known to elicit a biological response from the arterial endothelium consistent with the creation of new capillary beds in regions of ischemia. Such factors include the cell mitogens platelet-derived growth factors A and B and basic fibroblast growth factor. Although various patterns of pressure application may be used, pressures in excess of peak systolic pressure are necessary to produce the largest effect. Spatial distributions of pressure application are chosen to produce the most uniform distribution of elevated shear stress throughout the arterial tree of the lower extremity. It is been found that pressure applications previously referred to as " graded " or " wave like " are most efficient. Studies have also shown that to the arteries are able to inflate from a collapsed configuration during the period of a single heart cycle. It is therefore advantageous to apply the external compression on a cycle synchronized to the heart. It has also been shown that the greatest degree of emptying is produced when pressure in the external cuffs increases as rapidly as possible within a period of less than one-tenth of the second. Graded compression consists of applying pressure greatest at the calf and lowest at the proximal end of the compression region. The pressure difference between the distal and proximal ends of the compression region should be in the range of 50 mm of mercury. Wave-like or sequential compression is produced by inflating the distal portions of the cuff first and generating a wave of compression that propagates toward the heart. The speed of this wave should be comparable to the speed of wave propagation through the peripheral arteries.

Advantages and improvements over existing methods. Our studies have allowed us to optimize external compression of the lower extremities for the purpose of maximizing the stimulus to the arterial endothelium of the peripheral arteries in the leg. Others have attempted to optimize external compression on the notion that this can produce a reduction in systolic after load or diastolic augmentation. Numerous studies, however, have demonstrated that these effects are insufficient to produce significant cardiac benefits. More recently, studies in the literature have suggested that external compression of the lower extremities these to enhanced shear stress in the arteries of the coronary circulation and that this may be the mechanism for the beneficial effects of external compression. In both of those interpretations, the optimal compression cycle would be one that produces the greatest effect at the aortic root. Our new concept would

suggest that the optimal compression cycle should be determined by the hemodynamic effects seen in the lower extremity arteries, and would thereby lead to a different approach to the selection of the parameters associated with external compression.

Commercial applications. An external compression device of the type described herein would have benefit to anyone suffering from peripheral arterial disease in any organ or other part of the body. Patients who might otherwise be candidates for amputation could benefit from this method. It has already been proven effective in the relief of angina, and there is some evidence that it can enhance perfusion of the heart.

Companies that might be interested in this technology:
Aircast, Inc. (sponsor of the original research)
Jim Johnson (President)

Numerical Simulation of Enhanced External Counterpulsation

Part II: Hemodynamic Results

Karen E. Bottom, Edwin T. Ozawa, Xinshu Xiao, and Roger D. Kamm

Department of Mechanical Engineering

Fluid Mechanics Laboratory

Massachusetts Institute of Technology,

Cambridge, MA 02139

Short title: Simulation of EECP

Address for correspondence:

Roger D. Kamm

M.I.T. Room 3-260

77 Massachussetts Ave.

Cambridge, MA 02139

e-mail: rdkamm@mit.edu

voice: 617-253-5330

fax: 617-258-8559

Abstract

Enhanced external counterpulsation (EECP) is a noninvasive, counterpulsative method to provide temporary aid to the failing heart by sequentially inflating cuffs on the lower extremity out-of-phase with the left ventricle. The efficacy of EECP is dependent on the maximum external pressure applied by each cuff, the starting time of cuff inflation and deflation, the time between adjacent cuff inflations, and the total time to inflate and deflate the cuffs. Optimization of these parameters necessitates consideration of the hemodynamics created by EECP and the mode of action providing patient benefit. A distributed computational model has been developed that simulates cardiovascular hemodynamics during EECP. The model includes a 30-element distributed arterial system including the left ventricle, bifurcations, and peripheral arterial vessels. Effects of vessel collapse as external pressure is applied, arterial refilling on pressure release, changes in aortic pressure and cardiac output, and the level of shear stress generated in the arteries are each investigated. Device parameters are systematically varied to determine their effect on system performance. Results show significant collapse and shear augmentation throughout the arteries of the lower extremity. Performance is strongly influenced by the mean level of pressurization and the timing of cuff inflation, but less so by the relative timing and pressure differences between cuff segments.

Keywords: Enhanced external counterpulsation, cardiac assist, computational model, revascularization

Introduction

Enhanced external counterpulsation (EECP) is a non-invasive, counterpulsative procedure providing temporary support for the failing heart. EECP involves surrounding the lower half of a patient's body (lower abdomen, thighs, and calves) with inflatable cuffs that are pressurized and depressurized approximately out-of-phase with the left ventricle. While the aortic valve is closed (ventricular diastole), pressurization of the cuffs collapses the arteries causing the blood stored in the lower extremities to be directed retrograde toward the heart. The resultant increase in aortic diastolic pressure has been shown to increase blood flow to various organs, including the heart. Measurements by Applebaum et al. in the renal and carotid arteries indicate increases in mean flow velocities of 19% and 22%, respectively.[2] Although coronary perfusion is enhanced by EECP, studies indicate the extent of diastolic augmentation is relatively small. Just before the onset of ventricular ejection (systole), the cuffs are depressurized to atmospheric pressure and the collapsed arteries begin to refill. Cuff depressurization causes a rarefaction wave to propagate in the retrograde direction that reaches the heart during cardiac systole. As a result, cardiac afterload is decreased. As in the case of coronary perfusion enhancement, the benefits of afterload reduction are relatively small, and EECP has not found acceptance as a cardiac assist procedure.

Despite its lack of success as a means of cardiac assist, use of EECP has continued. Based initially on the success of clinical studies conducted in China, and more recently in the United States, EECP is now used as a treatment for patients suffering from cardiac ischemia and severe angina secondary to coronary disease.[1,11,19] In a study by Lawson et al., 17 out of 18 patients receiving EECP for as little as 36 one-hour

treatments reported improvement in anginal symptoms, despite prior medical and surgical therapy.[11] The results of a recent multi-center study involving 139 patients confirmed these findings and showed that EECP reduces exercise induced ischemia and angina.[3] A 1996 study by Lawson et al. also showed improved exercise tolerance in 22 out of 27 patients with chronic stable angina.[10] The mechanism by which patients accrue benefit from EECP treatments, however, remains unclear.

Mechanisms other than the purely mechanical ones can also be envisioned to explain the cardiovascular benefits of EECP. It has been widely demonstrated that the arterial and venous endothelia and smooth muscle cells are exquisitely sensitive to fluid dynamic shear stress and mechanical strain.[6,17] Results obtained from endothelial cell cultures suggest that shear stress can influence the synthesis and release of pro-angiogenic factors from endothelial or smooth muscle cells. Examples include the cell mitogens platelet-derived growth factors A and B and basic fibroblast growth factor.[7,8,13,14,15] Shear stress is also instrumental in the control of nitric oxide, endothelin-1, transforming growth factor β_1, and a host of others, many of which could contribute to coronary angiogenesis. In vivo studies also suggest a role for shear stress in wound-healing angiogenesis.[9] In a recent review, Soran et al. hypothesized that the beneficial effects of EECP might be a consequence of increased shear stress in the coronary vascular bed.[16] Here we propose that the vascular (endothelial and/or smooth muscle) cells of the lower extremity are a more likely source of these growth factors and cytokines since the enhancement in shear stress is far more dramatic there than in the coronary vessels, and the endothelial surface area is far greater. Consequently, we focus in this paper not only on the changes in pressure produced at the aortic root as it relates to

direct, mechanical cardiac effects and coronary blood flow, but also on arterial collapse and the augmentation of hemodynamic shear stress that accompany lower extremity compression.

Given this motivation, the work presented here concentrates on understanding the fundamental hemodynamics associated with EECP to determine how the operating parameters of the device influence its performance by a variety of measures. A cardiovascular fluid mechanics model is presented that simulates hemodynamics during operation of an EECP device. The underlying model theory is presented in Part I of this paper. This model differs from previous ones used to investigate EECP in that it represents the arterial system as a distributed, rather than lumped element network thus allowing for the realistic simulation of wave propagation phenomena, vessel collapse and refilling, and distribution of shear stresses in the entire arterial circulation.

Methods

The cardiovascular computer model consists of a distributed arterial system and boundary conditions to simulate the left ventricle, bifurcations, and peripheral vessels. A lumped parameter venous and pulmonary system is used only to calculate the initial hemodynamic state of the model based on the prescribed input parameters to the model. This initial state is used by the distributed arterial system to begin the simulation. The distributed arterial system contains twenty-eight main arteries or segments. The proximal and distal boundary conditions for the arterial system are, respectively, the left ventricle and the lumped parameter windkessel model for the finer branching peripheral vessels.

Details of the computational method and analytical equations used in the model are described in Part I of this paper; only changes to the model specific to EECP are presented here.

Modified Terminal Boundary Condition. The boundary condition for the terminal branch points, described in Part I, is modified to account for volume changes in the small peripheral vessels when external pressure is applied to the lower extremities. This is accomplished by using the externally applied pressure as the reference pressure for the capacitor in the windkessel model. Venous pressure is assumed constant for the purpose of these calculations. Consequently, the dynamics occurring on the venous side of the circulation, while potentially important, are not considered in the present calculations.

External Pressurization Scheme. A three-step *graded-sequential* compression procedure was employed in all the simulations presented here. In sequential compression, a wave of compression is applied to the vessels by inflating the three pressurization cuffs for the calves, thighs, and lower abdomen sequentially from ankle to groin. The pressure level applied by the cuffs decreases from calf to thigh, and from thigh to lower abdomen cuffs. In contrast to the emptying behavior characteristic of uniform compression, *sequential compression* produces a collapse in the vessels that proceeds from the foot toward the heart. Thus, the blood is effectively "milked" from the vessels in the lower extremities and does not pass through a constrictive throat as in uniform compression.[12] In *graded compression* the maximum level of pressure attained in each segment is greatest in the periphery and falls in the direction of the heart. The application of graded compression

also helps to eliminate the occlusive throat and, in combination with sequential pressure application, produces rapid and complete emptying of the vessels.[12,19]

The cuffs used to provide pressurization of the lower extremities in EECP are modeled as external pressure sources on the lower abdomen, thigh, and calf arteries. To simulate graded-sequential compression in the model, the arterial tree elements for the lower body are divided into three regions, shown in Fig. 1, representing the areas covered by the three pressurization cuffs in EECP.

External Pressurization Control Parameters. Clinical and computational studies have shown the efficacy of EECP is highly dependent on the mode of operation and parameter values used to control the device.[4] Thus, understanding the effect of individual EECP control parameters on the performance of the device is essential for achieving an optimal design. The inputs to the model are the control parameters governing the application of external pressure by the EECP cuffs. These parameters include the cuff inflation and deflation timings, the maximum pressure level applied externally to the vessels by each cuff, and the time delay of pressurization and depressurization between the calf, thigh, and lower abdomen cuffs for sequential compression. Table 1 shows a detailed description of the individual input control parameters governing external pressurization in the model.

In clinical practice, the application of external pressure during EECP is timed with the patient's electrocardiogram (ECG). In EECP, this process is accomplished by adjusting the relative timing of applied external pressure in each of the three compartments and the left ventricular contraction. For graded-sequential compression,

the pressure in each cuff rises linearly to it's maximum value over a time t_{tramp}, is held constant until a time T_{defl}, and then falls linearly over a time t_{ramp}. The calf, thigh, and lower abdomen cuffs are inflated at times T_{infl}, $T_{infl}+\Delta t_{seg}$, and $T_{infl}+2\Delta t_{seg}$, respectively. The maximum applied pressure is decreased between the calf and thigh cuffs and the thigh and lower abdomen cuffs as specified by P_{calf}, P_{th}, and P_{la}. The cuff deflation time, T_{defl}, is the same for all three cuffs to simplify the parameter study. The parameters used in the temporal application of external pressure during the heart cycle are shown in Fig. 2.

External Pressurization Measures of Merit. The effectiveness of enhanced external counterpulsation is assessed in terms of the following:

(1) augmentation of mean diastolic pressure, signifying increased coronary perfusion, and lowering of mean systolic pressure, signifying reduced left ventricular afterload, and
(2) elevation of shear stress and increased emptying of the arteries of the lower extremity.

Several *measures of merit* are chosen to quantify the effectiveness of EECP based on these criteria.

Mean Diastolic Pressure. The increase in diastolic pressure, or diastolic augmentation, is characterized by the mean diastolic pressure ratio:

$$MDP = \frac{\left[\frac{1}{T_D - T_S}\int_{T_S}^{T_D} P_{aortic}\,dt\right]_{compr} - \left[\frac{1}{T_D - T_S}\int_{T_S}^{T_D} P_{aortic}\,dt\right]_0}{\left[\frac{1}{T_D - T_S}\int_{T_S}^{T_D} P_{aortic}\,dt\right]_0} \quad (1)$$

where P_{aortic} is pressure at the aortic root, T_D and T_S are the times at which diastole and systole end, and the subscripts "compr" and "0" refer to cases with and without external compression, respectively. ***MDP*** is an indication of how diastolic pressure is increased with pressurization. All pressures are measured when the model has reached steady-state after 10 heart cycles.

Mean Systolic Pressure. The effect of EECP on systolic pressure is quantified using the mean systolic pressure ratio:

$$MSP = \frac{\left[\frac{1}{T_S}\int_0^{T_S} P_{aortic}\,dt\right]_{compr} - \left[\frac{1}{T_S}\int_0^{T_S} P_{aortic}\,dt\right]_0}{\left[\frac{1}{T_S}\int_0^{T_S} P_{aortic}\,dt\right]_0} \quad (2)$$

MSP is a measure of the extent of left ventricular afterload reduction with pressurization.

Emptying Effectiveness. The efficacy of EECP is highly dependent on the extent to which the arteries are emptied and refilled during each heart cycle. The blood volume emptied from the vessels corresponds to the amount of retrograde flow, and hence the amount of diastolic augmentation achieved by EECP. It also provides a measure of the

extent to which arterial diameter changes, and therefore relates to vessel wall strain. The emptying effectiveness parameter, ***EE***, is used to measure the efficiency of the emptying process for the vessels receiving pressurization. ***EE*** is calculated for a single vessel using the equation: has not been sufficient time for it to completely refill.

$$EE = \frac{\left[\int A dx\right]_0 - \left[\int A dx\right]_{compr}}{\left[\int A dx\right]_0} \tag{3}$$

where A is the cross-sectional area of the artery. The integrations are taken over the entire region of pressurization. For the "compr" case, arterial area is measured at maximum pressurization in diastole just prior to cuff deflation. The arterial area for case "0" is measured at the time step just preceding pressurization. Thus, the emptying effectiveness of the artery represents the extent of arterial collapse under maximum pressurization with respect to the state of the artery just prior to pressurization. The state of the artery prior to pressurization is considered since the artery may be partially collapsed if there has not been sufficient time for it to completely refill.

Shear Stress Index. An approximate measure of shear stress is defined, that accounts for the changes in cross-sectional area and flow velocity that accompany EECP. In the case of steady, fully-developed, laminar flow through a vessel of circular cross-section, wall shear stress could be computed as follows:

$$\tau_w = \mu \frac{4\overline{V}}{\sqrt{A/\pi}} \tag{4}$$

where $\overline{V}$ is the mean flow velocity. Recognizing that as an artery collapses, its cross-section will likely deviate from circular, and that the flow is clearly not fully-developed or steady, we will still assume to a rough approximation that

$$\tau_w \propto \mu \frac{\overline{V}}{\sqrt{A}} \tag{5}$$

A shear index, S, is defined as

$$S = \frac{\sum_{n=1}^{3} \tau_w}{\sum_{n=1}^{3} \tau_{w,o}} \tag{6}$$

where τ_w is the time integral of the wall shear stress for one cycle evaluated at the mid-point of the compression zone and $\tau_{w,o}$ is the same value with no external pressurization. The summation sign indicates that the values of τ_w and $\tau_{w,o}$ are summed over the three compression zones.

Results

Understanding the effect of individual parameters on the performance of the EECP device is essential for achieving an optimal design. Here, each parameter is

systematically varied in the model while holding all others constant. The results are presented in two ways to examine the two different mechanisms of action. In one, time-varying pressure at the radial artery is presented to demonstrate the reduction in systolic and increase in diastolic pressures, respectively. In the other, the impact of each individual parameter is presented in terms of a sensitivity matrix that shows the extent to which 20% variation (±10% from the baseline condition) influences each of the various measures of merit presented earlier.

All data presented in this section are taken from the tenth heart cycle of the model to ensure that the simulation has reached a steady state. A heart rate of 72 beats/min is used for all simulations.

Effects of EECP on aortic pressures. A base state was chosen, typical of conditions used clinically, from which the effects of various parameter variations could be studied. Values of the control parameters used for this base state are given in Table 1. Some judgement was exercised in parameter selection. Mean applied pressure was chosen at a level thought to produce a minimum of trauma to the patient while still providing a reasonable measure of benefit. The pressure increment between segments was viewed as sufficient to prevent proximal arterial collapse and a consequent impairment of vessel emptying while still providing ample pressure at the lower abdomen region to produce significant emptying. Consistent with the notion that arterial emptying should proceed at a speed comparable to the speed of the arterial pressure pulse (about 8 m/s in the peripheral arteries), the time delay between segment compressions was chosen to be approximately equal to the wave transit time through each of the pressurized

compartments. Pressure rise time, as shown by Bai et al., should be as short as possible.[5] Therefore, a value was chosen close to the practical lower limit.

Fig. 3 shows the radial pressure pulse computed by the model with and without graded-sequential external compression from the lower abdomen to the foot. In this case, pressure is applied by a three-compartment cuff with maximum pressures of 200, 150 and 100 mmHg along the lower leg, upper leg, and lower abdomen, respectively. Note that in this instance of arterial counterpulsation (pressure application during cardiac diastole and release of pressure during systole) systolic pressure is reduced while diastolic pressure is augmented, leading to the combined effects of reduced ventricular afterload and enhanced coronary blood flow.

The effectiveness of EECP can be viewed in terms of the measures of merit defined previously. These results are shown in Table 2. Numbers shown in the table correspond to the fractional change in each measure from the case without compression.

For this same condition of external compression, the time-varying arterial cross-sectional area and a measure proportional to the time-varying shear stress (see Eqn. (5)) are plotted for three locations (lower abdomen, thigh, and calf) in Fig. 4. During pressure application, the arteries collapse with sufficient speed to cause a flow reversal throughout much of the arterial network and a significant increase in vascular shear stress in the arteries of the lower extremity. The arteries in the lower abdomen and thigh (Figs. 4(a) and 4(b), respectively) refill rapidly upon pressure release, even rising to slightly above normal levels due to the strong compression wave generated and its reflection from the peripheral vascular bed. During refilling, shear stress attains levels roughly 3- to 4-fold higher than under normal conditions at all three locations. Features of particular interest

in the context of endothelial function are the high shear stresses of reversing sign, and the significant arterial wall strain due to arterial collapse.

Sensitivity matrix. One way to elucidate the relative effects of the various compression parameters is to establish the sensitivity matrix of Table 3. Considering that each measure of merit (*MM*) (e.g., mean diastolic pressure, ***MDP***) is a function of each of the adjustable parameters (*Y*) (e.g., mean applied pressure), then an entry in the table (*X*) represents the change in the measure of merit [$\Delta(MM)$] divided by the fractional change in the parameter value:

$$X = Y_{mean} \frac{\Delta(MM)}{\Delta Y} \tag{7}$$

Large values indicate strong correlations between the measure of merit and the particular parameter. For example, a 10% increase in mean applied pressure will produce a 7.92% increase in ***MDP***. This table is useful for identifying the parameters that, when varied, will have the greatest influence on the measure of interest.

While the dependencies are generally quite symmetric about the baseline case suggesting a nearly linear dependence, there are two notable exceptions. The time to initiate external compression (T_{infl}) selected for the baseline case was near the optimum in terms of mean systolic pressure. Thus, although T_{infl} has a strong influence on the effectiveness of EECP, changing it from the baseline case will not reap much benefit in ***MDP*** and ***MSP***; however, shear stress can be enhanced considerably. Second, the effect of mean applied pressure on the shear index was skewed in the sense that an increase in

pressure gave rise to a much greater increase in S than the decrease observed when pressure was reduced. This may reflect the synergistic effects of greater collapse and higher flow rates when applied pressure is increased. Mean applied pressure clearly has the greatest potential to enhance diastolic pressure and increase levels of shear stress, although increasing mean pressure probably has the largest negative impact on patient tolerance. Reducing pressure rise time would also be beneficial (except for the effect it has on arterial emptying), although this too may be determined largely by practical constraints. The results in Table 3 demonstrate the potential for controlling the mechanical events related to cardiac assist or vascular cell stimulation.

Discussion

The basic features of these numerical results are consistent with clinical observations during EECP. Compression beginning near the end of systole produces arterial collapse, sending a wave of retrograde flow up into the aorta, increasing pressure up as far as the aortic root and, presumably, augmenting coronary blood flow. When compression is released near the end of diastole, the arteries begin to refill, initiating a rarefaction wave that propagates toward the heart, reaching it at a point that produces systolic unloading. The extent of emptying of the leg arteries decreases toward the periphery, but corresponds to approximately half the normal arterial volume. Refilling to normal volumes is achieved in the most proximal arteries, but even at the levels of pressure used in these simulations, is incomplete in the lower leg. Increasing mean pressure applied to the calf up to 300 mmHg (results not shown) compromises refilling even further.

Recent clinical results showing that as little as one hour of treatment per day is sufficient to have a positive effect on cardiac function point to the importance of factors other than the obvious mechanical ones. Specifically, the well-documented effects of shear stress on endothelial or smooth muscle cell function are implicated. Shear stress is enhanced through a combination of flow augmentation and reduced arterial cross-sectional areas, up to levels more than four times normal arterial shear stress throughout much of the arterial system of the lower extremities. These high levels of shear occur during both antegrade and retrograde flow, giving rise to a strong oscillatory shear stimulus to the arterial endothelium. By comparison, the coronary vascular bed would experience much lower levels of shear augmentation. Increases in coronary shear stress can be roughly estimated by the relative increase in mean diastolic pressure at the aortic root, approximately 8% for the baseline conditions used in this study (Table 2). This, combined with the fact that the total endothelial surface area in the coronary beds is far less than in the lower extremities, suggest that the effects of shear stress stimulus in the latter would have the greater influence.

In previous models of EECP, the arteries were represented as collection of lumped elements and were therefore not capable of accurately capturing many of the phenomena associated with wave propagation through the arterial network and arterial collapse.[4] As seen in Fig. 4, the onset of compression at the lower leg sends a surge of blood toward the heart, producing the peak in area in the thigh (see e.g., t=3.60 s in Fig. 4(b)) and the lower abdomen (t=3.64 s in Fig. 4(a)) just prior to compression of these regions. The abrupt fall in cross-sectional area in the calf (beginning at t=3.56 s, Fig. 4(c)) is followed by an equally abrupt rise in area, before the area decreases more

consistently as pressure is maintained. The low frequency oscillation occurring in the iliac artery (t=2.9 - 3.2 s, Fig. 4(a)) is evidence of wave reflection from the proximal end of the aorta, causing some refilling while pressure is still maintained. These waves are highly damped, however, and are not seen in the thigh or calf regions.

These results, in terms of the magnitude of the effect observed in arterial blood flow and pressure, are consistent with previous observations. In the multi-center study, the hemodynamic effects of EECP were monitored by determining the ratio of peak diastolic pressure to peak systolic pressure, referenced to end-diastolic pressure.[3] Using the aortic blood pressure trace (data not shown), this ratio is 1.24 for our standard case simulation compared to an average of 1.41 in the multi-center trial. The greater values achieved in patients reflects the higher range of pressures (up to 300 mmHg) used in the clinical study. In the Suresh study, most effects (e.g., change in cardiac output, ratio of retrograde to antegrade aortic flow) had nearly reached their maximal effect when the diastolic-to-systolic pressure ratio reached values in the range of one to 2.[18]

We chose to study a range of pressures somewhat below those currently used clinically in recognition of the relatively high number of adverse experiences reported by patients receiving EECP. In the multi-center study, 54.9% of the patients experienced adverse effects, with the majority of these being device-related. The number of device-related adverse effects was reduced nearly 4-fold (from 37 to 10) when pressures were decreased from 300 mmHg to 75 mmHg. Our results suggest that significant hemodynamic effects, especially in terms of enhancing arterial shear stress and arterial wall strain, can be achieved with the use of considerably lower pressures, with mean values in the range of 150 mmHg.

Given the exquisite sensitivity of endothelial cells to shear stress in vitro, it is likely that the flow alterations caused by EECP would significantly alter the profile of gene expression throughout the vessels of the lower extremity. Since these alterations affect nearly the entire arterial network below the waist, the potential for elevated synthesis and secretion of various cytokines and growth factors is considerable. If released into the circulation, many of these would remain active for the short time it takes to reach the coronary vasculature and could potentially exert an influence there. Some, NO for example, would likely exert an effect only in the peripheral bed of the lower extremities due to its short half-life. Although speculative, this possibility has not previously been considered and clearly deserves further study.

In terms of designing optimal protocols for EECP, it is critically important to understand the mechanism by which myocardial function is improved. In particular, parameter variations that optimize the traditional measures of merit (reduction in systolic pressure and increase in diastolic pressure) are not always consonant with the desire to maximize the magnitude and spatial extent of changes in arterial shear stress in the lower extremity. These issues will need to be better understood before a rationale design of the EECP protocol is possible.

Acknowledgements

The authors would like to thank AirCast, Inc. for their financial and technical support in this research.

References

[1]Amsterdam, E.A., Banas, J., Cartley, J.M., et al. Clinical assessment of external pressure circulatory assistance in acute myocardial infarction. *American Journal of Cardiology*, Vol. 45, 349, 1990.

[2]Applebaum, R.M., Kasliwal, R., Tunick, P.A., Konecky, N., Katz, E., Trehan, N., Kronzon, I. Sequential external counterpulsation increases cerebral and renal blood flow. *American Heart Journal*, Vol. 133, No. 6, 611-615, June 1997.

[3]Arora, R.R., Chou, T.M., Jain, D., Fleishman, B., Crawford, L., McKiernan, T., Nesto, R.W. The multicenter study of enhanced external counterpulsation (MUST-EECP): effect of EECP on exercise-induced myocardial ischemia and anginal episodes. *Journal of the American College of Cardiology*, Vol. 33, No. 7, 1833-1840, June 1999.

[4]Bai, J., Wu, D., Zhang, J. A Simulation Study of External Counterpulsation. *Computers in Biology and Medicine*, Vol. 24, No. 2, 145-156, 1994.

[5]Bai, J., Ying, K., Jaron, D. Cardiovascular responses to external counterpulsation: a computer simulation. *Medical and Biological Engineering and Computing*, Vol. 30, 317-323, 1992.

[6]Davies, P.F. Mechanisms involved in endothelial responses to hemodynamic forces. *Atherosclerosis*, Vol. 131, Suppl., S15-S17, June 1997.

[7]Diamond, S.L., Sharefkin, J.B., Dieffenbach, C., Frasier-Scott, K., McIntire, L.V., and Eskin, S.G. Tissue plasminogen activator messenger RNA levels increase in cultured human endothelial cells exposed to laminar shear stress. *Journal of Cell Physiology*, Vol. 143, 364-71, 1990.

[8]Hseih, H.J., Li, N.Q., Frangos, J.A. Shear stress increases endothelial platelet-derived growth factor mRNA levels. *American Journal of Physiology*, Vol. 260, H642-H646, 1991.

[9]Ichioka, S., Shibata, M., Kosaki, K., Sata, Y., Harii, K., Kamiya, A. Effects of shear stress on wound-healing angiogenesis in the rabbit ear chamber. *Journal of Surgical Research*, Vol. 72, 29-35, 1997.

[10]Lawson, W.E., Hui, J.C., Zheng, Z.S., Burgen, L., Jiang, L., Lillis, O., Oster, Z., Soroff, H., Cohn, P. Improved exercise tolerance following enhanced external counterpulsation: cardiac or peripheral effect? *Cardiology*, Vol. 87, No. 4, 271-275, July-August 1996.

[11]Lawson, W.E., Hui, J.C., Soroff H.S., Zheng, Z., et al. Efficacy of enhanced external counterpulsation in the treatment of angina pectoris. *American Journal of Cardiology*, Vol. 70, No. 9, 859-862, 1992.

[12]Lueptow, R.M., Karlen, J.M., Kamm, R.D., Shapiro, A.H. Circulatory Model Studies of External Cardiac Assist by Counterpulsation. *Cardiovascular Research*, Vol. 15, No. 8, 443-455, August 1981.

[13]Malek, A.M., Gibbons, G.H., Dzau, V.J. and Izumo, S. Fluid shear stress differentially modulates expression of genes encoding basic fibroblast gwoth factor and platelet-derived growth factor B chain in vascular endothelium. *Journal of Clinical Investigation*, Vol. 92, 2013-2021, 1993.

[14]Mason, I.J. The ins and outs of fibroblast growth factors. *Cell*, Vol. 78, No. 4, 547-552, August 1994.

[15]Mitsumata, M., Fishel, R.S., Nerem, R.M., Alexander, R.W., Berk, B.C. Fluid shear stress stimulates platelet-derived growth factor expression in endothelial cells. *American Journal of Physiology*, Vol. 265, No. 1 Pt. 2, H3-H8, July 1993.

[16]Soran, A.U., Crawford, L.E., Schneider, V.M., and Feldman, A.M. Enhanced external counterpulsation in the management of patients with cardiovascular disease. *Clinical Cardiology*, Vol. 22, No. 3, 173-178, 1999.

[17]Sumpio, B.E., Hemodynamic forces and the biology of the endothelium: signal transduction pathways in endothelial cells subjected to physical forces in vitro. *Journal of Vascular Surgery*, Vol. 13, No. 5, 744-746, May 1991.

[18]Suresh, K., Simandl, S., Lawson, W.E., Hui, J.C., Lillis, O., Burger, L., Guo, T., Cohn, P.F. Maximizing the hemodynamic benefit of enhanced external counterpulsation. *Clinical Cardiology*, Vol. 21, No. 9, 649-653, September 1998.

[19]Zheng, Z.S., Li, T.M., Kambic H., et al. Sequential external counterpulsation (SECP) in China. *Transactions of the American Society of Artificial Internal Organs*, Vol. 29, 599-603, 1983.

Table 1. External Pressurization Input Control Parameters. All times referenced to the beginning of cardiac systole.

Parameter	*Description*	*Baseline Values*
T_{infl}	Time from onset of cardiac cycle at which pressure starts to rise	0.20 s
T_{defl}	Time to begin deflation of cuffs from maximum external pressure	0.72 s
T_{card}	Period of cardiac cycle	0.86 s
P_{calf}	Maximum external pressure applied to calf vessels	200 mmHg
P_{th}	Maximum external pressure applied to thigh vessels	150 mmHg
P_{la}	Maximum external pressure applied to lower abdomen vessels	100 mmHg
Δt_{seg}	Time interval between inflations of adjacent cuff regions with the proximal region always pressurized first	0.03 s
t_{ramp}	Time it takes pressure to rise to and fall from its maximum value	0.03 s
ΔP_{seg}	Pressure difference between cuffs (pressure always increasing in the direction of the foot)	50 mmHg
P_m	Average applied pressure in the three cuff regions	150 mmHg

Table 2. Values for each of the measures of merit for the baseline conditions given in Table 1.

	Values under baseline conditions
MDP	0.0782
MSP	-0.0238
EE	0.373
S	4.22

Table 3. Sensitivity matrix. Each numerical value represents the change in the particular measure of merit divided by the fractional change in the parameter as defined in Eqn. (7).

	P_m	ΔP_{seg}	T_{ramp}	Δt_{seg}	T_{infl}
MDP	0.0792	-0.0110	-0.0084	-0.0067	-0.0694
MSP	-0.0299	0.0122	0.0035	-0.0016	0.0014
EE	-0.229	0.088	-0.028	-0.011	0.262
S	11.91	-0.8164	-0.1180	0.4529	2.599

Figure Captions

Fig. 1. Division of lower arterial tree elements into three pressurization regions for EECP model. Figure is drawn to scale.

Fig. 2. Application of external pressure with time during the heart cycle. Parameter values as given in Table 1.

Fig. 3. Pressure at the radial artery showing the effect of external compression shown over several cardiac cycles following the onset of EECP. Note the reduction in systolic pressure and increase in diastolic pressure. Parameter values as given in Table 1.

Fig. 4(a), (b), (c). Cross-sectional area plotted vs. time for several cardiac cycles following the onset of EECP at the midpoint of the lower abdomen, thigh, and calf compression zones, respectively, normalized with respect to the cross-sectional area without external compression at 100 mmHg (A_o). Light lines: no external compression. Dark lines: with external compression.

Fig. 4(d), (e), (f). A measure of arterial wall shear stress [Eqn. (5)] plotted vs. time for several cardiac cycles following the onset of EECP at the midpoint of the lower abdomen, thigh, and calf compression zones, respectively. Magnitude is increased by more than 3-fold (much more in the lower abdomen) and flow reversal is evident. Light lines: no external compression. Dark lines: with external compression.

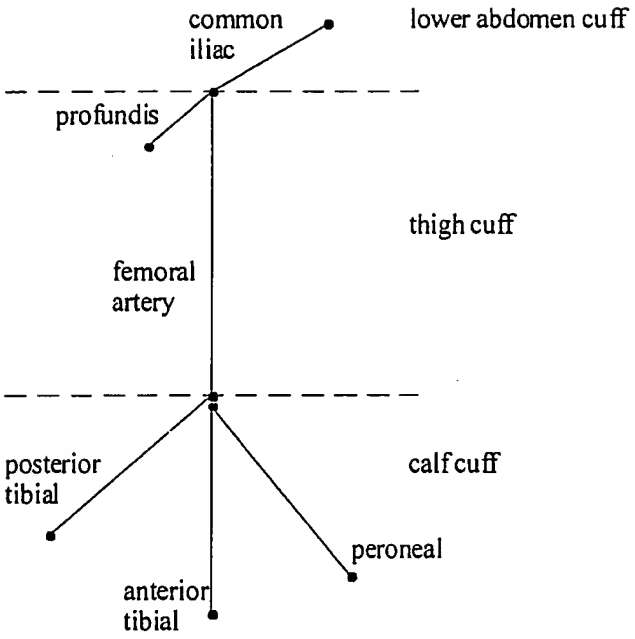
common
iliac
lower abdomen cuff
profundis
thigh cuff
femoral
artery
posterior
tibial
calf cuff
peroneal
anterior
tibial

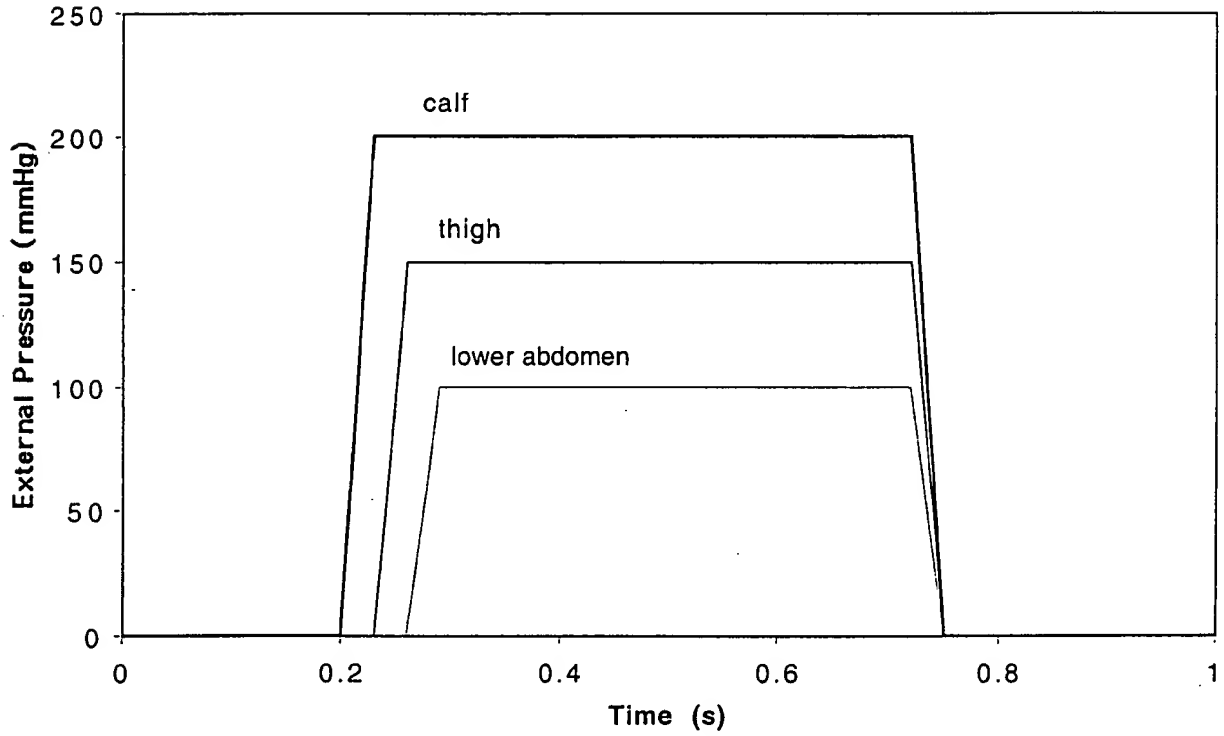
250
200
150
100
50
0
External Pressure (mmHg)
calf
thigh
lower abdomen
0
0.2
0.4
0.6
0.8
1
Time (s)

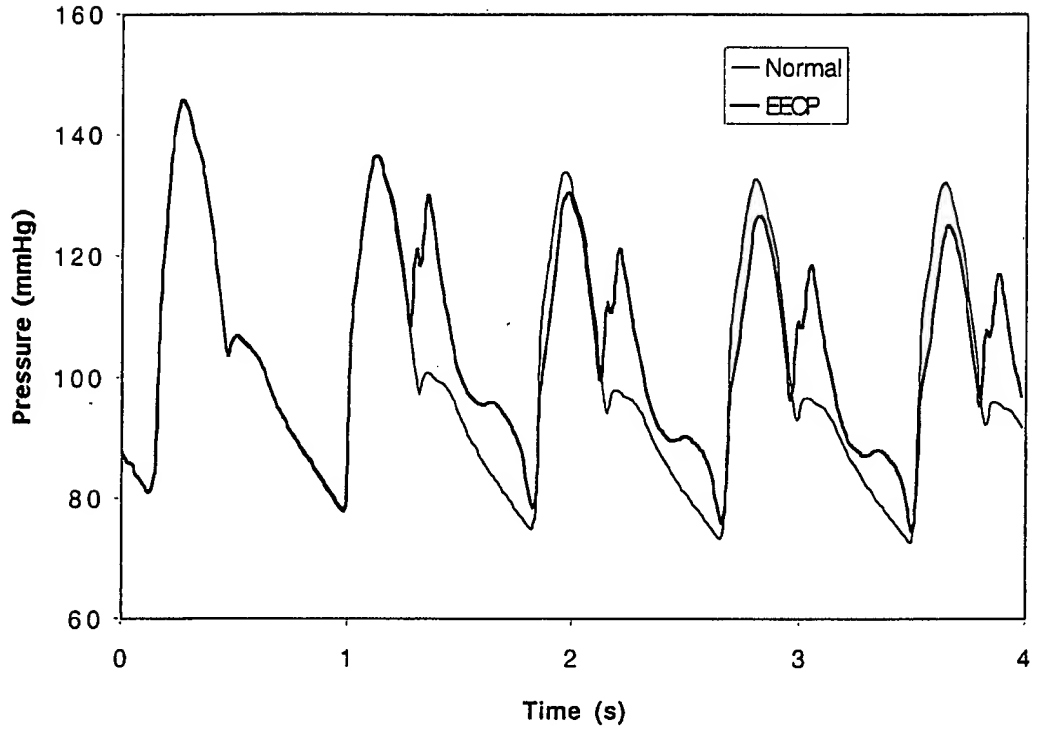
160
140
120
100
80
60
Pressure (mmHg)
0
1
2
3
4
Time (s)
Normal
EECP

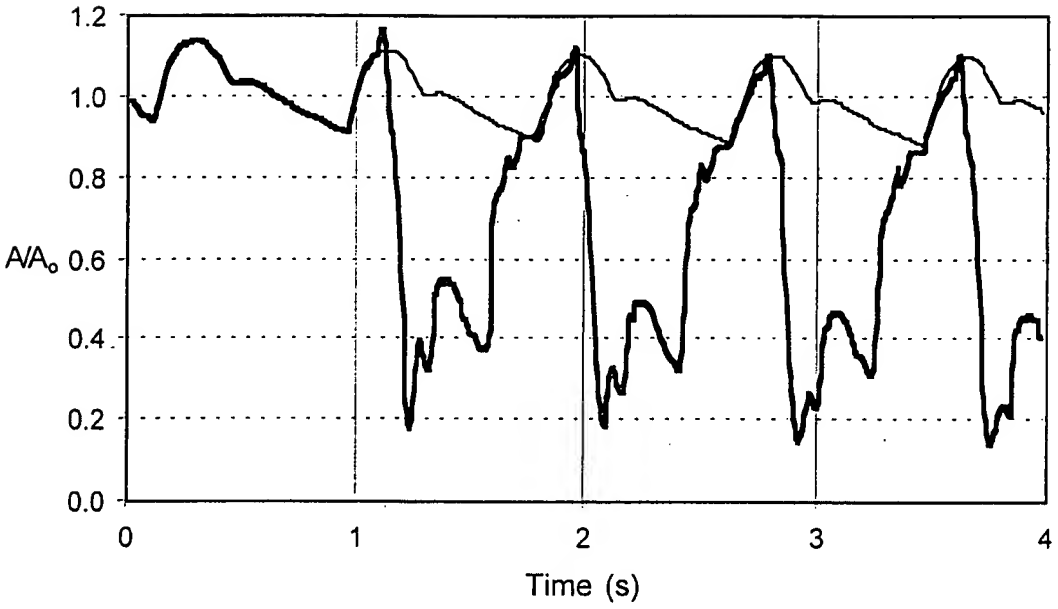
1.2
1.0
0.8
A/A$_o$ 0.6
0.4
0.2
0.0
0
1
2
3
4
Time (s)

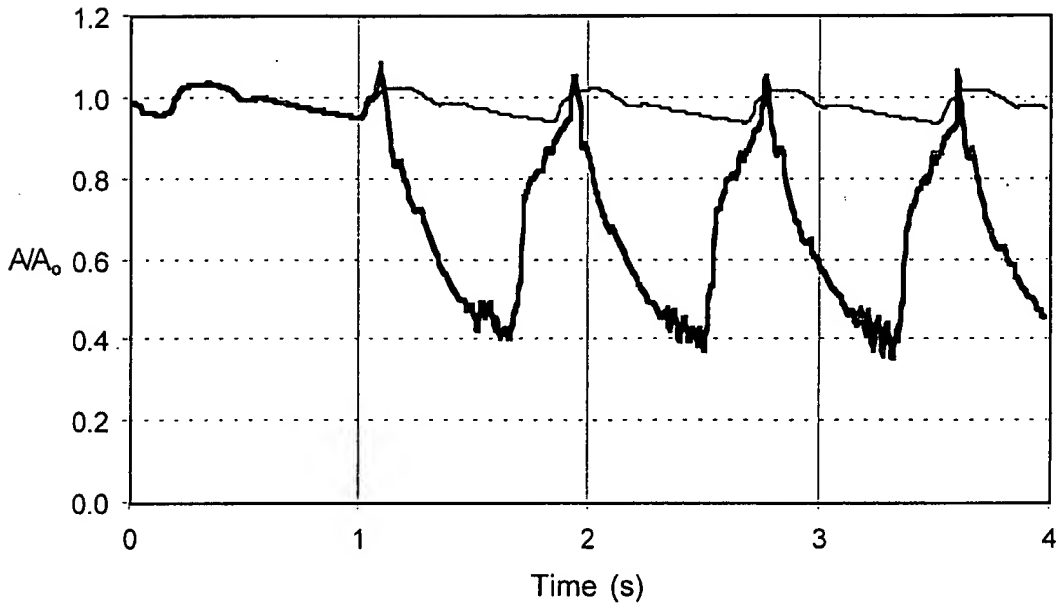
1.2
1.0
0.8
A/A$_o$ 0.6
0.4
0.2
0.0
0
1
2
3
4
Time (s)

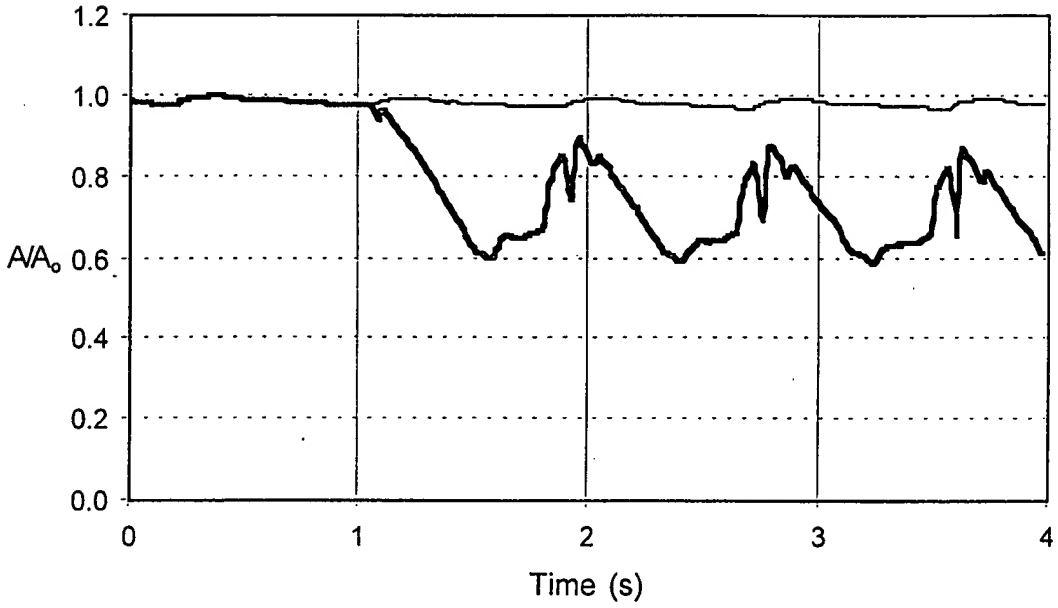
1.2
1.0
0.8
A/A$_o$ 0.6
0.4
0.2
0.0
0
1
2
3
4
Time (s)

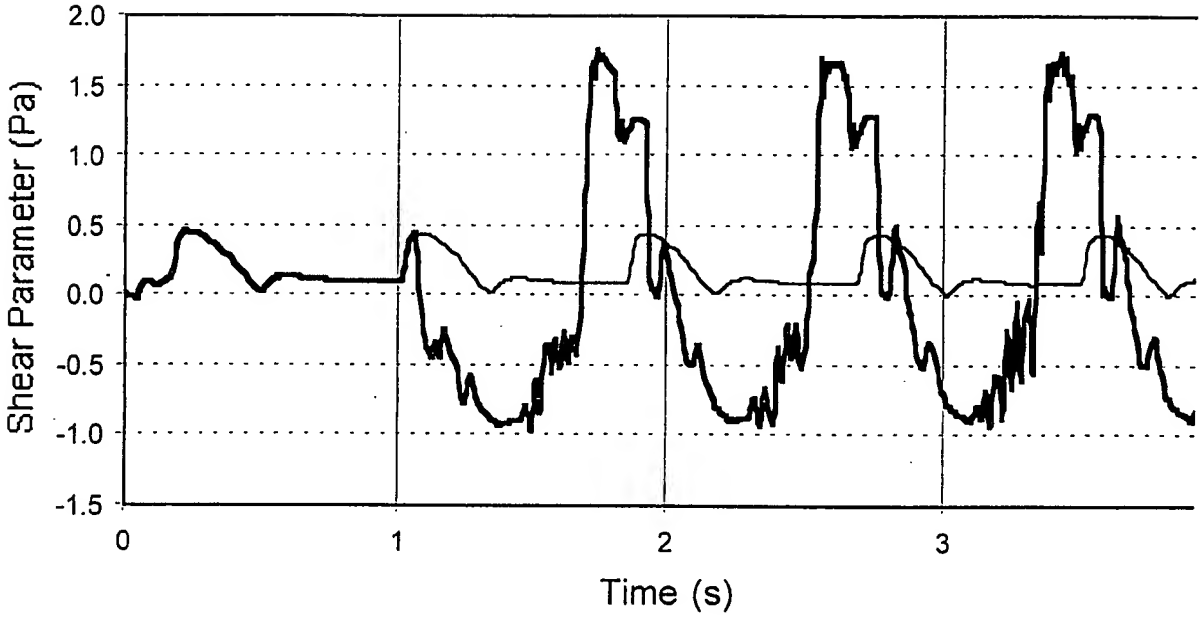
2.0
1.5
1.0
0.5
0.0
-0.5
-1.0
-1.5
Shear Parameter (Pa)
0
1
2
3
Time (s)

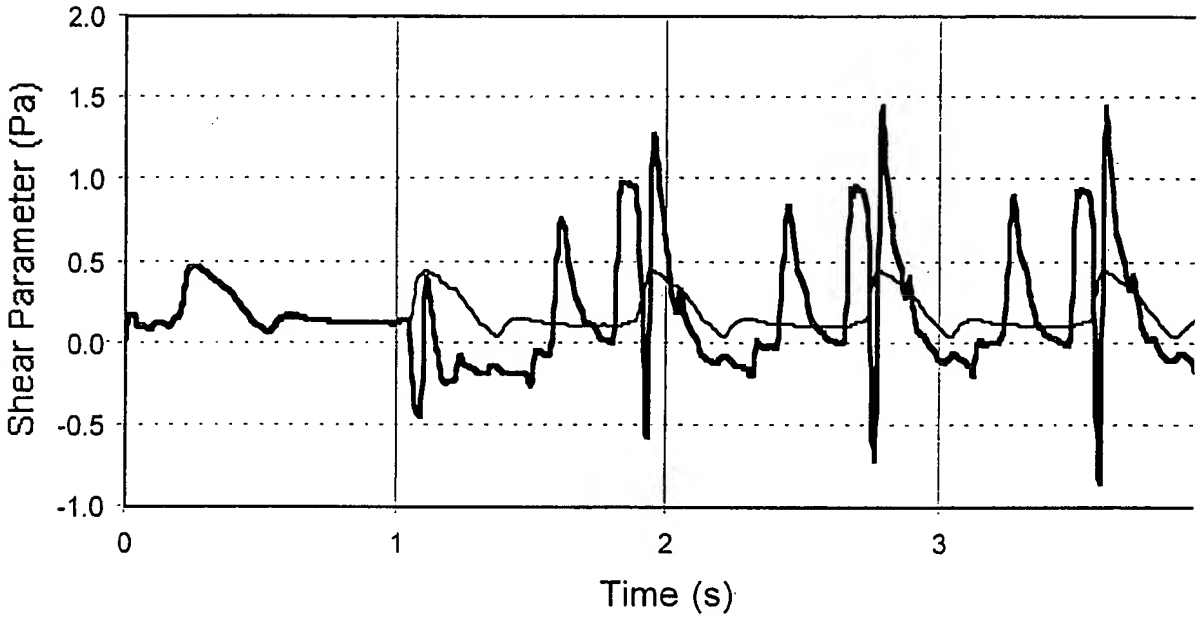
2.0
1.5
1.0
0.5
0.0
-0.5
-1.0
Shear Parameter (Pa)
0
1
2
3
Time (s)